Available online at www.sciencedirect.com
ScienceDirect
International Journal of Pharmaceutics 352 (2008) 287–293
INTERNATIONAL JOURNAL OF PHARMACEUTICS
www.elsevier.com/locate/ijpharm

Pharmaceutical Nanotechnology

Loading of curcumin into macrophages using lipid-based nanoparticles

Keitaro Sou, Shunsuke Inenaga, Shinji Takeoka, Eishun Tsuchida *

Advanced Research Institute for Science and Engineering, Waseda University, Tokyo 169-8555, Japan

Received 3 July 2007; received in revised form 28 August 2007; accepted 21 October 2007
Available online 1 November 2007

Abstract

Curcumin (1,7-bis(4-hydroxy-3-methoxyphenyl)-1,6-heptadiene-3,5-dione, Cm) is a natural compound which possesses antioxidant, anti-inflammatory and anti-tumor ability. Here, phospholipid vesicles or lipid-nanospheres embedding Cm (CmVe or CmLn) were formulated to deliver Cm into tissue macrophages through intravenous injection. Cm could be solubilized in hydrophobic regions of these particles to form nanoparticle dispersions, and these formulations showed ability to scavenge reactive oxygen species as antioxidants in dispersions. At 6 h after intravenous injection in rats via the tail vein (2 mg Cm/kg bw), confocal microscopic observations of tissue sections showed that Cm was massively distributed in cells assumed as macrophages into the bone marrow and spleen. Taken together, these results indicate that the lipid-based nanoparticulates provide improved intravenous delivery of Cm to tissues macrophages, specifically bone marrow and splenic macrophages in present formulation, which has therapeutic potential as an antioxidant and anti-inflammatory.

Keywords: Nanoparticles; Liposomes; Bone marrow; Macrophage; Antioxidant; Drug delivery

1. Introduction

Because of the significant phagocytic ability of the mononuclear phagocyte system (MPS) to nanoparticles *in vivo*, drug delivery which targets macrophages can be reasonably achieved by using nanoparticles. Recent studies indicated that macrophages relate with various diseases associated with inflammation and the macrophage targeting may open new therapeutic approaches for controlling the diseases (Chellat et al., 2005; Zeisberger et al., 2006; Schmid and Varner, 2007).

Curcumin (1,7-bis(4-hydroxy-3-methoxyphenyl)-1,6-heptadiene-3,5-dione, Cm) (Fig. 1) is a natural compound isolated from the root of *Curcuma longa* that has been shown to exhibit antioxidant, anti-inflammatory and anti-tumor abilities (Kunchandy and Rao, 1990; Singh and Aggarwal, 1995; Kuo et al., 1996; Shishodia et al., 2005; Sharma et al., 2005). Cm has been demonstrated to have scavenger ability against reactive oxygen species (ROS), such as superoxide anion ($O_2^{\bullet -}$), hydrogen peroxide (H_2O_2) and nitric oxide (NO), both *in vitro* and *in vivo* (Kunchandy and Rao, 1990). In addition, it has been reported to be a potent inducer of heme oxygenase-1 in vascular endothelial cells (Motterlini et al., 2000). These properties contribute to the protection of cells and tissue from oxidative stress. Further, anti-inflammatory ability of Cm is induced by the suppression of nuclear factor-kappa B (NF-κB) activation, which results in the inhibition of synthesis of inducible nitric oxide synthase (iNOS) in macrophages (Pan et al., 2000). Thus, macrophages can be a therapeutic targeted cellular component for Cm.

Oral Cm administration as a cancer therapy in phase I clinical studies in humans produced minimal side effects (Cheng et al., 2001; Sharma et al., 2004). However, the clinical pharmacokinetics studies revealed maximum Cm plasma levels in the range of only 1.8–11 nM in patients, even for oral administration of several grams of Cm per day. Thus, the current conclusion on Cm is that it has poor bioavailability when orally administered. This unsatisfactory pharmacokinetics of oral administration is not restricted to Cm, but is also observed for various lipophilic drug candidates.

A promising approach to developing improved delivery systems lipophilic drugs employs lipid-based carriers such as

* Corresponding author. Tel.: +813 5286 3120; fax: +813 3205 4740.
E-mail addresses: ksou@waseda.jp (K. Sou), eishun@waseda.jp (E. Tsuchida).

0378-5173/$ – see front matter © 2007 Elsevier B.V. All rights reserved.
doi:10.1016/j.ijpharm.2007.10.033

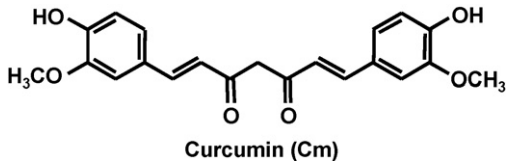

Fig. 1. Structure of curcumin. This compound is insoluble in water because of strong hydrophobicity of diketo moiety.

micelles, vesicles (liposomes), and nano- or microspheres, which can solubilize lipophilic drugs in self-assembling processes. Cm is known to interact with phospholipids or surfactants to solubilize in aqueous dispersions (Began et al., 1999; Tønnesen, 2002; Bruzell et al., 2005). Recently, some investigators have advanced this research to incorporate complexes of Cm with phospholipids in drug delivery systems (Li et al., 2005; Kunwar et al., 2006; Maiti et al., 2007). In immunohistochemical studies, Li et al. observed antiangiogenesis effect following intravenous injection of Cm-liposomes, which suppressed pancreatic carcinoma growth in murine xenograft models (Li et al., 2005). More recently, Maiti et al. reported that intraperitoneal injection of Cm–phospholipid complex has better hepatoprotective activity, owe to its superior antioxidant property, than free Cm (Maiti et al., 2007). These reports indicated that the therapeutic potential of Cm would be enhanced by the development of efficient drug delivery system.

Recently, we found that surface modification of vesicles with L-glutamic acid, *N*-(3-carboxy-1-oxopropyl)-, 1,5-dihexadecyl ester (SA) and poly(ethylene glycol) (PEG)-lipid increases the distribution of vesicles into bone marrow macrophage when injected in small doses (Sou et al., 2007). This finding is applied for the intravenous delivery of Cm to tissue macrophages in this study. Here, nano-sized vesicles containing Cm (CmVe) and lipid-nanospheres (CmLn) were prepared and characterized. Furthermore, distribution of Cm in organs after intravenous injection in rats was observed. We show that these nanoparticle systems would be available to deliver Cm to tissues macrophages, specifically bone marrow and splenic macrophages in present system.

2. Materials and methods

2.1. Materials

1,2-Dimyristoyl-*sn*-glycero-3-phosphocholine (DMPC) and L-glutamic acid, *N*-(3-carboxy-1-oxopropyl)-, 1,5-dihexadecyl ester (SA) were purchased from Nippon Fine Chemical Co. Ltd. (Osaka, Japan); 1,2-distearoyl-*sn*-glycero-3-phosphoethanolamine-*N*-[monomethoxy poly(ethylene glycol) (5000)] (PEG-DSPE) was purchased from NOF Co. (Tokyo, Japan). Soybean oil was purchased from Kanto Chemical Co. (Tokyo, Japan). Curcumin (Cm) was purchased from SIGMA (St. Louis, MO, USA). 8-Amino-5-chloro-7-phenylpyrid[3,4-*d*]pyridazine-1,4-(2H,3H) dione sodium salt (L-012), hypoxanthine, xanthine oxidase, and superoxide dismutase (SOD, 3400 U/mg), were purchased from Wako Pure Chemical Industries (Tokyo, Japan).

2.2. Preparation of CmVe

Lipid powder of DMPC/SA/PEG-DSPE (10/1/0.06, molar ratio) and Cm were dissolved in the mixed solvent system of *t*-butyl alcohol and benzene (1/1, v/v) and then lyophilized to obtain mixed lipid powder containing Cm. The lyophilized powder was hydrated in physiological saline at 70 mg mL^{-1} for 30 min under stirring by a vortex mixer. The dispersion was subjected to extrusion (final pore size of the filter: 0.2 μm, Isopore®, Millipore, Tokyo, Japan) and finally filtered through sterilized filters (pore size: 0.2 μm Dismic, Toyo Roshi, Tokyo, Japan) to obtain fine-sized Cm-vesicles (CmVe). Sample preparation for animal experiment was performed under sterilized conditions.

2.3. Preparation of CmLn

To prepare the Cm lipid-nanosphere formulation (CmLn), Cm was dissolved in soybean oil (10 mg mL^{-1}) at 150 °C, and then mixed with lipid powder comprising DMPC/SA/PEG-DSPE (10/1/0.06, molar ratio) dissolved in soybean oil (280 mg mL^{-1}) at 60 °C. This mixed solution was introduced into 2.5% glycerin solution under vigorously stirring with a wing stirrer (1200 rpm) and continuously stirred for 30 min to obtain crude lipid-microsphere dispersion. The dispersion was subjected to extrusion to control the size of the lipid-nanosphere (final pore size of the filter: 0.2 μm, Isopore®, Millipore, Tokyo, Japan) and finally passed through sterilized filters (pore size: 0.2 μm Dismic, Toyo Roshi, Tokyo, Japan) to obtain CmLn. Sample preparation for animal experiment was performed under sterilized conditions.

2.4. Characterization of CmVe and CmLn

The concentration of Cm in CmVe and CmLn was determined from calibration curves of absorbance at 420 nm prepared in ethanol, and the concentration of phospholipid was determined using a phospholipid assay kit (Phospholipid C Test Wako, Wako Pure Chemical, Tokyo Japan). The diameter of the resulting CmVe and CmLn was determined with a COULTER submicron particle analyzer (N4SD, Coulter, Hialeah, FL), and represented as an average diameter ± standard deviation (S.D.). The zeta(ζ)-potential was determined with a Zeta-Sizer Nano ZS (Malvern, MA, USA). Florescence imaging was carried out with excitation at 488 nm on a confocal scanning microscope (Olympus IX70, Tokyo, Japan) equipped with an ArKr ion laser system (Yokogawa) and recorded with image analysis software (IPLab version 3.5 for Macintosh, Scanalytics, Inc., VA, USA). Transmission electron microscopy (TEM) was carried out using a negative staining technique. Briefly, equivolumes of the sample and 2% phosphotungstic acid solution were mixed, and then a drop of mixed solution was allowed to settle on a carbon-coated copper grid for 1 min. Excess sample was removed by filter paper, dried in a desiccator, and visualized using a JEOL JEM-1011/100 kV (JEOL, Tokyo Japan).

2.5. Chemiluminescence assay

ROS scavenge ability of CmVe was evaluated by the generation of $O_2^{\bullet -}$ in a hypoxanthine and xanthine oxidase system. L-012 (50 μM) was used for chemiluminescence probe to detect $O_2^{\bullet -}$ according to Nishinaka et al. (1993). Xanthine oxidase, L-012, and CmVe were mixed together in test tube and $O_2^{\bullet -}$ generation was started by the addition of hypoxanthine. The final concentrations of regents were fixed at hypoxanthine, 0.5 mM; xanthine oxidase, 25 mU/mL; and L-120, 50 μM; CmVe was supplied in the concentration range 1–100 μM. Chemiluminescence was counted for 3 min after addition of hypoxanthine using an AccuFLEX Lumi400 from ALOKA (Tokyo, Japan). Ve, having the same lipid concentration with CmVe, was tested with the same procedure to determine the effect of lipid components. In addition, SOD, which is a popular $O_2^{\bullet -}$ scavenger, was tested with the same procedure to serve as a reference for the $O_2^{\bullet -}$ scavenging ability.

2.6. Animal experiments

Animal experiments were performed under the regulations for Animal Experimentation at Waseda University and were approved by the Steering Committee for Animal Experimentation at Waseda University. Male Wister rats (200–218 g) were anesthetized with 2% isoflurane (VedCo, St Joseph, MO, USA) in 100% oxygen gas. Samples were injected into the tail vein at 1 mL/min. Each rat received a total dose of Cm: 2 mg/kg as dispersion of CmVe or CmLn ($n = 5$). The blood sample was collected just before injection, and various time after injection to monitor the circulation level of blood cells. At 6 h after injection, the animals were scarified to collect bone marrow, liver, and spleen. The organs were fixed in 10% formaldehyde, sectioned, fixed on glass slides with 2% agar solution, and observed under a confocal scanning microscope (Olympus IX-70).

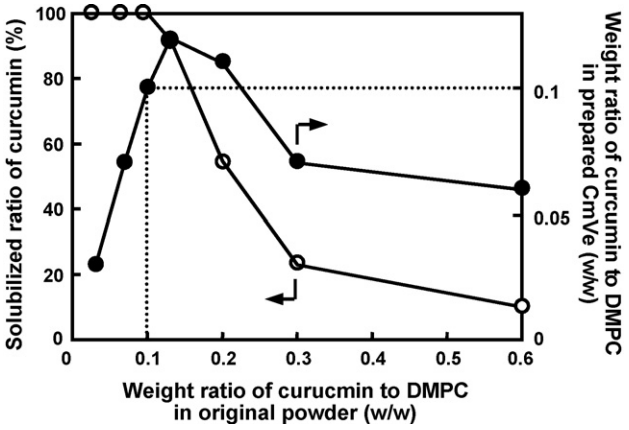

Fig. 2. Solubilization capacity of DMPC-vesicles for curcumin.

3. Results

3.1. Preparation and characterization of CmVe

All DMPC, SA, PEG-DSPE, and Cm compounds were successfully dissolved in mixed solvent of *t*-butyl alcohol and benzene (1/1, volume ratio) and the lyophilized powder was employed for the preparation of vesicles. Initially, we applied various amounts of Cm in order to determine the maximum capacity of vesicles to stably immobilize the Cm. As shown in Fig. 2, when the weight ratio of Cm to DMPC was below 0.1, vesicles could completely solubilize the Cm in dispersion of vesicles. When the weight ratio of employed Cm in the origi-

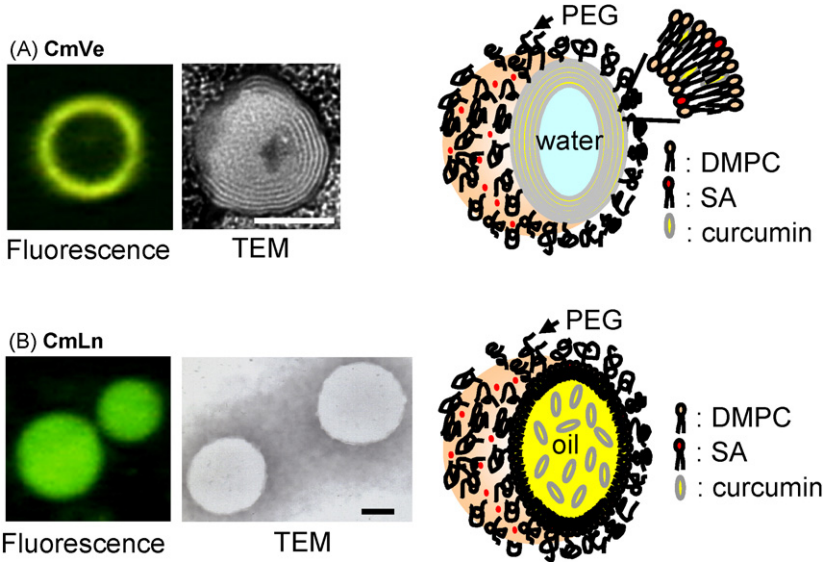

Fig. 3. Structural characterization of (A) DMPC-vesicles comprising curcumin (CmVe) and (B) lipid-nanosphere comprising curcumin (CmLn). Confocal scanning microscopic images (left) and transmission electron micrographs (TEM) (right) of CmVe and CmLn. Confocal scanning microscopic images were taken before extrusion to submicron size to enable observation of the structure within resolution of a confocal microscope. These images indicate the localization of Cm in vesicles and lipid-sphere with diameter of ca. 10 μm. Bars in TEM represent 100 nm. Illustrations are estimated structures of CmVe and CmLn.

Table 1
Diameter and ζ-potential of CmVe and CmLn with and without SA

Particle type	Composition of lipids (molar ratio)	Diameter (nm)	ζ-potential[a] (mV)
CmVe	DMPC/PEG-DSPE (10/0.06)	193 ± 75	−1.99 ± 1.86
	DMPC/SA/PEG-DSPE (10/1/0.06)	187 ± 53	−21.1 ± 1.88
CmLn	DMPC/PEG-DSPE (10/0.06)	219 ± 95	0.018 ± 1.95
	DMPC/SA/PEG-DSPE (10/1/0.06)	217 ± 93	−19.8 ± 0.28

[a] ζ-potential was measured in 10 mM phosphate buffer solution (pH 7.4, NaCl 20 mM).

nal powder was increased above 0.1, an excess fraction of Cm formed an orange solid in dispersion medium during hydration. To control the size of vesicles resulting in the decreasing of solubilized ratio of Cm, the solid Cm was filtrated out in the subsequent extrusion procedure. Therefore, we determined that the capacity of the present vesicles to stably solubilize Cm was 0.1 in weight ratio of Cm to DMPC, a value which is equivalent to 16 mol% Cm in the DMPC membrane. Thus, we determined the stable formulation of vesicles solubilizing Cm in their bilayer membrane to be DMPC/SA/PEG-DSPE/Cm (10/1/0.06/1.9, molar ratio), which is applied for the following experiments as CmVe. We confirmed that 97% of Cm was present in CmVe fraction separated by ultracentrifugation, indicating that little Cm was isolated from Ve in prepared dispersion.

Confocal scanning microscopic observation indicated that the Cm was located in the membrane of vesicles, but not in the inner aqueous phase, while TEM observation showed that the CmVe have an origolamellar structure, which is typically comprised of three to six layers. One representative vesicle is shown in Fig. 3A. The ζ-potential of CmVe was determined to be -21.1 ± 1.88 mV at pH 7.4 and its diameter was 187 ± 53 nm (Table 1). This data showed that the CmVe is a nano-sized anionic particle. The ζ-potential of vesicle prepared without SA was -1.99 ± 1.86 mV, indicating that the incorporation of SA results in an anionic surface. Based on these results, we estimated the structure of CmVe as illustrated in Fig. 3A, where PEG and SA express their physicochemical characters on the surface of CmVe, and Cm locates in the multilayer bilayer membrane. Spectroscopic data further indicate that the location of Cm is in the bilayer membrane. As shown in Fig. 4A, the spectra of CmVe dispersion showed a peak with three compartments. The λ_{max} was observed at 401 nm at 10 °C, where the dispersion was orange rather than yellow. With increasing temperature, the peak at 401 nm decreased and the peak at 420 nm increased to where the color of dispersion changed to yellow. Plotting the absorbance at 420 nm by temperature showed that the absorbance of 420 nm was critically increased between 20 and 30 °C (Fig. 4B). This range corresponded to the gel–liquid crystalline phase transition temperature of DMPC (23 °C) (Pownall et al., 1977), suggesting that the molecular state of Cm is influenced by the phase state of the bilayer membrane. This observation also supported by the fact that Cm is located in the bilayer membrane.

3.2. Preparation and characterization of CmLn

Regarding the preparation of CmLn, the solubility of the Cm in soybean oil was limited to the maximum solubilization of Cm, which has a solubility of approximately 10 mg mL^{-1} at preparation condition (around 25 °C). The same lipid formulation with CmVe [DMPC/SA/PEG-DSPE (10/1/0.06, molar ratio)] was applied for CmLn. The soybean oil solution was injected into 2.5% glycerin solution under stirring. Subsequently, the dispersion was passed through a membrane filter to control the size of CmLn. The incorporation of SA contributed to the anionic surface of CmLn (ζ-potential: −19.8 mV) indicating that the anionic head group of SA is located on the surface of the CmLn

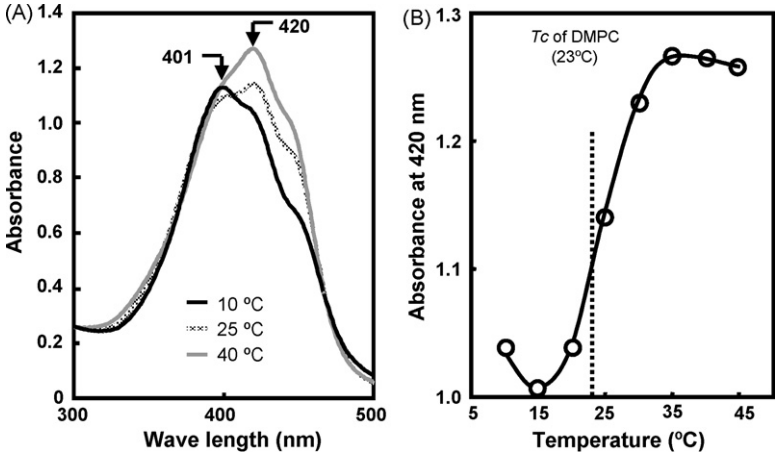

Fig. 4. Spectral property of CmVe dispersion with temperature. (A) Raw spectra at 10, 25, and 40 °C. (B) Absorbance at 420 nm plotted according to temperature. Absorbance of Cm critically changes in range of the gel–liquid crystalline phase transition temperature (T_c, 23 °C) of DMPC membrane, indicating that Cm is embedded in membrane.

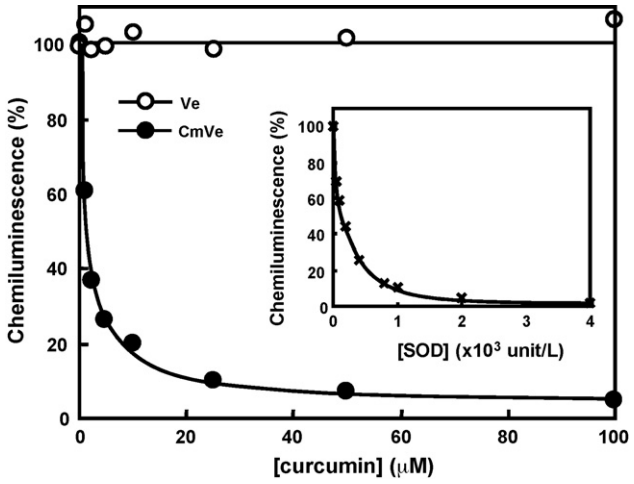

Fig. 5. Scavenging superoxide anion ($O_2^{\bullet -}$) by CmVe as a function of concentration of Cm. $O_2^{\bullet -}$ was produced by hypoxanthine (0.5 mM) and xanthine oxidase (25 mU/mL) system and detected by a chemiluminescence probe L-120 (50 μM). Vesicles without Cm (Ve) are being use as a control. Small panel shows the comparable experiment with SOD.

(Table 1). Confocal scanning microscopic observation indicated that the Cm was located inside the oil phase of Lm, while TEM observation indicated a spherical shape without an inner aqueous phase (Fig. 3B). Based on dynamic light scattering measurement, the diameter of CmLn was determined to be 217 ± 93 nm in dispersion state (Table 1).

3.3. ROS scavenge ability

As shown in Fig. 5, depending on the concentration of Cm, CmVe showed the ability to scavenge generated $O_2^{\bullet -}$ from hypoxanthine and xanthine oxidase system. Based on these data, we determined that the concentration of CmVe required to reduce 50% of chemiluminescence of L-012 by $O_2^{\bullet -}$ was 1.8, and 25 μM is required to reduce 90% of chemiluminescence of L-012 by $O_2^{\bullet -}$, as summarized in Table 2. As comparative index of $O_2^{\bullet -}$ scavenging ability, SOD which ability was defined as unit, was applied in the same $O_2^{\bullet -}$ generation system. As shown in the small panel in Fig. 5 and in Table 2, 160 units/L SOD reduced 50% of chemiluminescence of L-012, and 1050 units/L SOD reduced 90% of chemiluminescence of L-012. Thus, we roughly estimated that the $O_2^{\bullet -}$ scavenger ability in 1.8–25 μmol range of Cm in present formulation of CmVe was comparable to the 160–1050 range of SOD units. DMPC vesicles that consisted of saturated phospholipids and saturated SA were not reactive to $O_2^{\bullet -}$. These data indicate that the present nanoparticulate formulations potentially have ROS scavenger ability.

Table 2
Scavenger ability of CmVe or vesicles without Cm (Ve) to superoxide anion ($O_2^{\bullet -}$) generated from hypoxanthine and xanthine oxidase system

Scavengers	IC_{50}[a]	IC_{90}[a]
CmVe	1.8 μM	25 μM
Ve	na	na
SOD	160 units/L	1050 units/L

[a] IC_{50} and IC_{90} are concentration of Cm to scavenge 50 and 90% of $O_2^{\bullet -}$ (na = not active).

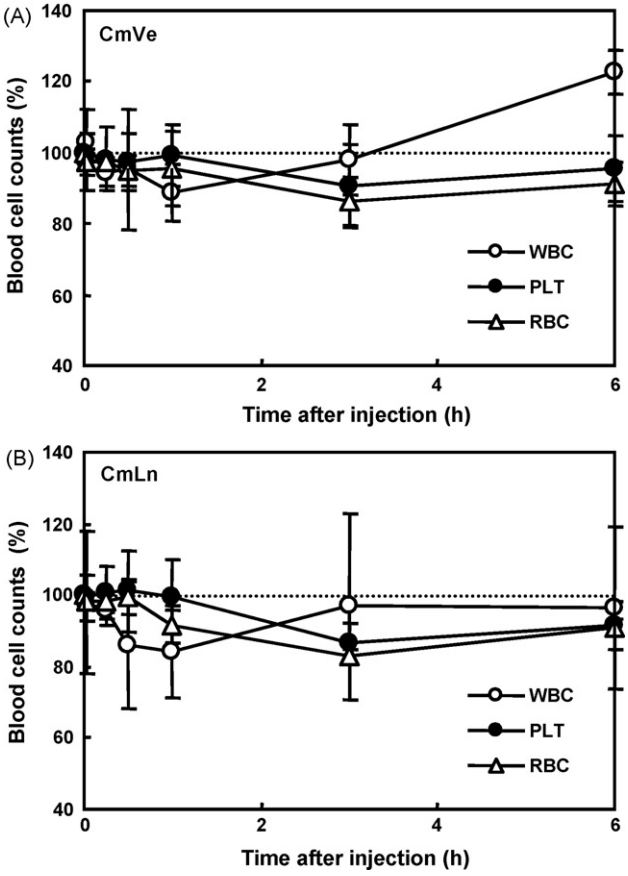

Fig. 6. Profiles of blood cell counts after intravenous infusion of (A) CmVe dispersion or (B) CmLn dispersion in rats. Each rat received 2 mg Cm/kg bw. Percentages are blood cell counts before injection of sample. WBC: white blood cells, PLT: platelets, RBC: Red blood cells.

3.4. Intravenous delivery and distribution in organs

Prepared CmVe or CmLn with SA were intravenously injected in rats to monitor the injection response of blood cells and observe organ distribution. All rats ($n = 5$) received CmVe or CmLn were survived for 6 h after injection. As shown in Fig. 6, no acute response to injection of these formulations was observed in circulating blood cells. In rats receiving CmVe or CmLn, white blood cells (WBC) tended to gradually decrease to 89 ± 8 or 84 ± 13% until 1 h, and then returned to baseline levels. Upper recovery to baseline levels was observed in CmVe at 6 h, but was not observed in CmLn. As for red blood cells (RBC) and platelets (PLT), the circulating level tended to decrease in a similar manner until 3 h, and then returned to baseline. At 6 h, bone marrow, liver, and spleen samples were collected for observation of the distribution of Cm in these tissues. As shown in Fig. 7, confocal scanning microscopy indicated that the Cm emitting yellow fluorescence was located in these tissues. This observation indicated intravenous injection of Cm using present lipid-based nanoparticles could facilitate the delivery of Cm into macrophages especially in bone marrow and spleen.

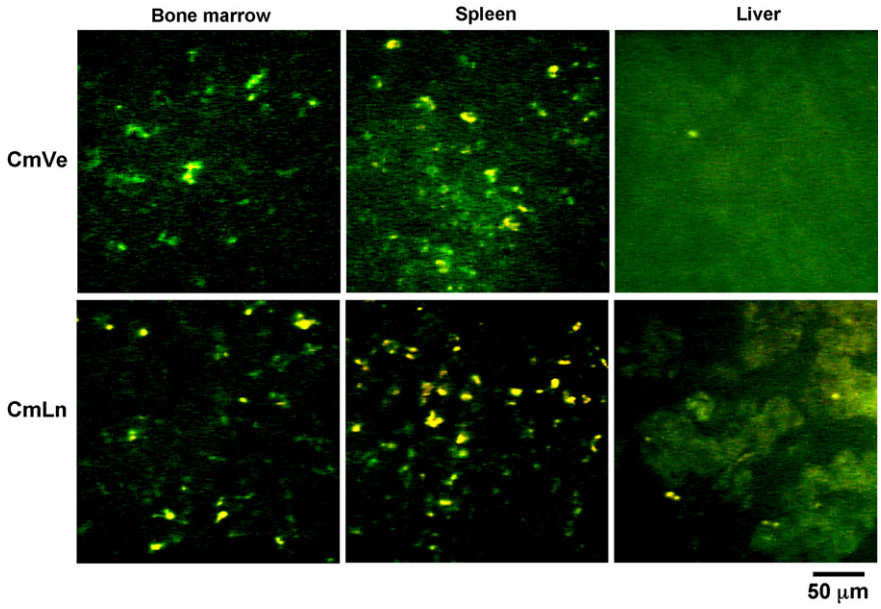

Fig. 7. Confocal scanning images of bone marrow, spleen, and liver collected from rat that received CmVe or CmLn dispersion (2 mg Cm/kg bw) 6 h after intravenous infusion. Yellow fluorescence indicates the distribution of Cm in organs.

4. Discussion

As Cm is a water-insoluble compound, Cm is conventionally administered orally, which has low bioavailability. The present study offered stable intravenous formulations using lipid-based nanoparticles. The binding constant for the interaction of Cm with egg and soy phosphatidylcholine was reported to be 3.26×10^5 and $2.64 \times 10^5\ M^{-1}$, respectively (Began et al., 1999), and that of phosphatidylcholine liposomes containing cholesterol was $2.5 \times 10^4\ M^{-1}$ (Kunwar et al., 2006). In our preliminary examination to determine the components of the bilayer membrane, vesicles that consisted of 1,2-dipalmitoyl-*sn*-glycero-3-phosphocholine and cholesterol (1/1, molar ratio) could solubilize much less Cm in bilayer membrane (below 3 wt.% of Cm to lipids) than DMPC vesicles, and the mixing examination of each component indicated that the low affinity of Cm to cholesterol causes the low solubilized capacity of bilayer membrane containing cholesterol (data not shown). Thus, we used DMPC without cholesterol to stably solubilize Cm. It has been reported that six molecules of phosphatidylcholine could bind one molecule of Cm (Began et al., 1999). As shown in Fig. 2, the maximum solubilization capacity of DMPC to Cm was determined to be approximately 10 wt.% and it was calculated that one Cm was fixed by 5.4 molecules of DMPC. These data are consistent with previous report (Began et al., 1999). In terms of preparation techniques, it should be considered that excess Cm formed solid precipitate which could be removed by filtration; however, as shown in Fig. 2, too much excess Cm decreased the solubilized amount of Cm. In the case of CmLn, the solubilization of Cm in employed oil was a factor for determining the maximum Cm content. Present soybean oil could solubilize Cm at approximately $10\ mg\ mL^{-1}$ in preparation conditions.

Confocal scanning microscopic observation clearly indicated that Cm was solubilized in the bilayer membrane of vesicles or the inner oil phase of lipid-nanosphere in the present preparation procedure. TEM observation showed the oligolamellar membrane structure of CmVe (Fig. 3A). The spectroscopic analysis also indicated that the location of Cm is in the bilayer membrane (Fig. 4). In contrast, we could not find lamellar membrane structure in CmLn (Fig. 3B). ζ-potential measurement indicated that the carboxyl group of SA is located on the surface to characterize the surface with anion (Table 1). Thus, we identified two kinds of characterized anionic particles solubilizing Cm in their hydrophobic region as CmVe and CmLn. We have identified that surface modification of phospholipid vesicles with two compounds, SA and PEG-DSPE, cooperatively increases the distribution of vesicles into bone marrow macrophages (Sou et al., 2007).

As a therapeutic potential, CmVe showed scavenger ability against the ROS in several μM ranges (Fig. 5 and Table 2). It has been suggested that Cm is a potent agent for the suppression of septic or hemorrhagic organ failure (Lukita-Atmadja et al., 2002; Madan and Ghosh, 2003; Kaur et al., 2006; Siddiqui et al., 2006). Macrophages are target cells in such inflammation because they produce various mediators such as cytokines and ROS that promote inflammation following oxidative damage. Therefore, we were interested in the distribution of Cm in organs, in which the fluorescence of Cm was useful to detect the Cm in organs as shown in Fig. 7. At 6 h after injection, organ distribution of Cm in the present particulate system clearly indicated that the cellular components assumed to be macrophages are responsible for the uptake, especially in bone marrow and spleen. The competition of splenic uptake to bone marrow uptake would be more significant in rat model than that in previous pharmacokinetic study of vesicles containing SA in a rabbit model, because the rat spleen has about nine times larger capacity for uptake of vesicles compared with rabbit spleen (Sou et al., 2005, 2007). In liver, the relative high background fluorescence might

be due to the diffuse distribution of Cm. It is known that albumin can bind Cm when the binding constant is in the 10^4–10^5 M^{-1} range (Kunwar et al., 2006; Pulla Reddy et al., 1999; Barik et al., 2003). As this binding constant of albumin to Cm is equal to that of phospholipids, it is speculated that a fraction of Cm might be transferred from vesicles to serum albumin. The cellular uptake was not obvious in liver. Further pharmacokinetic study is necessary in order to determine the quantitative distribution of Cm in whole body. In present study, we indicated that the loading of Cm into tissue macrophages, mainly bone marrow and splenic macrophages, could be achieved in rats. In addition to the ROS scavenger ability, this system can be expected to efficiently suppress the NF-κB activation to inhibit the synthesis of iNOS in macrophages (Pan et al., 2000). These events should be a therapeutic benefit for treatment with oxidative injury and inflammation.

5. Conclusions

Two nanoparticles embedding Cm have been offered for intravenous injection of Cm. These nanoparticulate formulations could deliver Cm into tissue macrophages, specifically bone marrow and splenic macrophages in rats. This intravenous delivery system of Cm using lipid-based nanoparticles may be available for antioxidant and anti-inflammatory therapies.

Acknowledgements

This work was partly supported by the Japanese Ministry of Education, Culture, Sports, Science and Technology, through a Grant-in-Aid for Scientific Research (B) (17300162, 2005). The authors gratefully acknowledge Dr. William T. Phillips and Dr. Beth Goins (UTHSCSA) for suggestion and discussion for this research.

References

Barik, A., Priyadarsini, K.I., Mohan, H., 2003. Photophysical studies on binding of curcumin to bovine serum albumin. Photochem. Photobiol. 7, 597–603.

Began, G., Sudharshan, E., Udaya Sankar, K., Appu Rao, A.G., 1999. Interaction of curcumin with phosphatidylcholine: a spectrofluorimetric study. J. Agric. Food Chem. 47, 4992–4997.

Bruzell, E.M., Morisbak, E., Tønnesen, H.H., 2005. Studies on curcumin and curcuminoids. XXIX. Photoinduced cytotoxicity of curcumin in selected aqueous preparations. Photochem. Photobiol. Sci. 4, 523–530.

Chellat, F., Merhi, Y., Moreau, A., Yahia, L'H., 2005. Therapeutic potential of nanoparticulate systems for macrophage targeting. Biomaterials 26, 7260–7275.

Cheng, A.L., Hsu, C.H., Lin, J.K., Hsu, M.M., Ho, Y.F., Shen, T.S., Ko, J.Y., Lin, J.T., Lin, B.R., Ming-Shiang, W., Yu, H.S., Jee, S.H., Chen, G.S., Chen, T.M., Chen, C.A., Lai, M.K., Pu, Y.S., Pan, M.H., Wang, Y.J., Tsai, C.C., Hsieh, C.Y., 2001. Phase I clinical trial of curcumin, a chemopreventive agent, in patients with high-risk or pre-malignant lesions. Anticancer Res. 21, 2895–2900.

Kaur, G., Tirkey, N., Bharrhan, S., Chanana, V., Rishi, P., Chopra, K., 2006. Inhibition of oxidative stress and cytokine activity by curcumin in amelioration of endotoxin-induced experimental hepatoxicity in rodents. Clin. Exp. Immunol. 145, 313–321.

Kunchandy, E., Rao, M.N.A., 1990. Oxygen radical scavenging activity of curcumin. Int. J. Pharm. 58, 237–240.

Kunwar, A., Barik, A., Pandey, R., Priyadarsini, K.I., 2006. Transport of liposomal and albumin loaded curcumin to living cells: an absorption and fluorescence spectroscopic study. Biochim. Biophys. Acta. 1760, 1513–1520.

Kuo, M.L., Huang, T.S., Lin, J.K., 1996. Curcumin, an antioxidant and antitumor promoter, induces apoptosis in human leukemia cells. Biochem. Biophys. Acta. 1317, 95–100.

Li, L., Braiteh, F.S., Kurzrock, R., 2005. Liposome-encapsulated curcumin. In vitro and in vivo effects on proliferation, apoptosis, signaling, and angiogenesis. Cancer 104, 1322–1331.

Lukita-Atmadja, W., Ito, Y., Baker, G.L., McCuskey, R.S., 2002. Effect of curcuminoids as anti-inflammatory agents on the hepatic microvascular response to endotoxin. Shock 17, 399–403.

Madan, B., Ghosh, B., 2003. Diferuloylmethane inhibits neutrophil infiltration and improves survival of mice in high-dose endotoxin shock. Shock 19, 91–96.

Maiti, K., Mukherjee, K., Gantait, A., Saha, B.P., Mukherjee, P.K., 2007. Curcumin-phospholipid complex: preparation, therapeutic evaluation and pharmacokinetic study in rats. Int. J. Pharm. 330, 155–163.

Motterlini, R., Foresti, R., Bassi, R., Green, C.J., 2000. Curcumin, an antioxidant and anti-inflammatory agent, induces heme oxygenase-1 and protects endothelial cells against oxidative stress. Free Radic. Biol. Med. 28, 1303–1312.

Nishinaka, Y., Aramaki, Y., Yoshida, H., Masuya, H., Sugawara, T., Ichimori, Y., 1993. A new sensitive chemiluminescence probe, L-012, for measuring the production of superoxide anion by cells. Biochem. Biophys. Res. Commun. 193, 554–559.

Pan, M.N., Lin-Shiau, S.Y., Lin, J.K., 2000. Comparative studies on the suppression of nitric oxide synthase by curcumin and its hydrogenated metabolites through down-regulation of IkappaB kinase and NFkappaB activation in macrophages. Biochem. Pharmacol. 60, 1665–1676.

Pownall, H.J., Morrisett, J.D., Gotto Jr, A.M., 1977. Composition-structure-function correlations in the binding of an apolipoprotein to phosphatidylcholine bilayer mixtures. J. Lipid Res. 18, 14–23.

Pulla Reddy, A.C., Sudharshan, E., Appu Rao, A.G., Lokesh, B.R., 1999. Interaction of curcumin with human serum albumin—a spectroscopic study. Lipids 34, 1025–1029.

Schmid, M.C., Varner, J.A., 2007. Myeloid cell trafficking and tumor angiogenesis. Cancer Lett. 250, 1–8.

Sharma, R.A., Euden, S.A., Platton, S.L., Cooke, D.N., Shafayat, A., Hewitt, H.R., Marczylo, T.H., Morgan, B., Hemingway, D., Plummer, S.M., Pirmohamed, M., Gescher, A.J., Steward, W.P., 2004. Phase I clinical trial of oral curcumin: biomarkers of systemic activity and compliance. Clin. Cancer Res. 10, 6847–6854.

Sharma, R.A., Gescher, A.J., Steward, W.P., 2005. Curcumin: the story so far. Eur. J. Cancer 41, 1955–1968.

Shishodia, S., Sethi, G., Aggarwal, B.B., 2005. Curcumin: getting back to the roots. Ann. N.Y. Acad. Sci. 1056, 206–217.

Siddiqui, A.M., Cui, X., Wu, R., Dong, W., Zhou, M., Hu, M., Simms, H.H., Wang, P., 2006. The anti-inflammatory effect of curcumin in an experimental model of sepsis is mediated by up-regulation of peroxisome proliferator-activated receptor-gamma. Crit. Care Med. 34, 1874–1882.

Singh, S., Aggarwal, B.B., 1995. Activation of transcription factor NF-kappa B is suppressed by curcumin (diferuloylmethane). J. Biol. Chem. 270, 24995–25000.

Sou, K., Goins, B., Takeoka, S., Tsuchida, E., Phillips, W.T., 2007. Selective uptake of surface-modified phospholipid vesicles by bone marrow macrophages in vivo. Biomaterials 28, 2655–2666.

Sou, K., Kilpper, R., Goins, B., Tsuchida, E., Phillips, W.T., 2005. Circulation kinetics and organ distribution of Hb-vesicles developed as a red blood cell substitute. J. Pharmacol. Exp. Ther. 312, 702–709.

Tønnesen, H.H., 2002. Solubility, chemical and photochemical stability of curcumin in surfactant solutions. Studies of curcumin and curcuminoids, XXVIII. Pharmazie 57, 820–824.

Zeisberger, S.M., Odermatt, B., Marty, C., Zehnder-Fjällman, A.H.M., Ballmer-Hofer, K., Schwendener, R.A., 2006. Clodronate-liposome-mediated depletion of tumour-associated macrophages: a new and highly effective antiangiogenic therapy approach. Br. J. Cancer 95, 272–281.